Biochimica et Biophysica Acta 897 (1987) 93–111
Elsevier

BBA 73369

A model for accelerated uptake and accumulation of sugars arising from phosphorylation at the inner surface of the cell membrane

R.J. Naftalin and P.M. Smith

Department of Physiology, King's College London, Strand, London (U.K.)

(Received 26 August 1986)

Key words: Active transport; Sugar transport; Transport model; Thermodynamics

A model transport system for cellular accumulation of sugar coupled to phosphorylation is described. Sugar permeates the cell membrane via a passive facilitated transport system. On the inside surface of the membrane the bound sugar is either phosphorylated to form impermeable hexose phosphate, which is released into the intracellular solution, or released directly into the cytosol. Sugar may be regenerated from hexose phosphate in the cytosol via a phosphatase reaction. The reduction of the proportion of sites on the inner membrane surface occupied by permeable sugar, caused by the kinase reaction, increases both net and unidirectional passive inflow and reduces both net and unidirectional exit of sugar, thereby permitting large stationary state gradients of free sugar to be maintained between the cytosol and bathing solution. In cells where there is a high passive membrane permeability to free sugar, steady-state accumulation of free sugar within the cytosol, linked to metabolism is inexplicable in terms of conventional transport kinetics based on equilibrium thermodynamic assumptions. This phenomenon is analysed in terms of non-equilibrium stationary state flows of ligands via a probability network. The effects of metabolism on exchange transport are also examined. The model provides a framework to explain how sugar transport is loosely coupled to phosphorylation in mammalian epithelial cells, adipocytes, yeasts and bacteria, so that a high rate of substrate accumulation is maintained without requiring a reduction in the intracellular concentration of permeable substrate below that in the external solution.

Introduction

In a number of microbial, plant and animal cells systems sugar transport is linked to intracellular metabolism and unrelated to ion gradients across the cell membranes. Examples of such systems may be found in renal cortical and small intestinal epithelial cells, in insulin-treated rat adipocytes, in baker's yeast and in the phosphotransferase systems of many bacteria.

Correspondence: R.J. Naftalin, Department of Physiology, King's College London, Strand, London WC2R 2LS, U.K.

Sugar accumulation

In mammalian tissues

Free 2-D-deoxyglucose, 2-D-deoxygalactose and D-galactose accumulate within rabbit [1–3] and hamster [4] renal tubular epithelial cells to higher concentrations than in the bathing solutions by a process linked to cell metabolism. This accumulation is unrelated to ion gradients, not inhibited by ouabain, but is inhibited by metabolic poisons, e.g., dinitrophenol, cyanide, or the transport inhibitor, phloretin [1–4].

However, there are several results which do not support the view that transport is completely cou-

pled to phosphorylation namely: (i) the rate of 2-deoxyglucose uptake into hamster kidney slices is faster than the rate of accumulation of 2-deoxyglucose phosphate [4]. (ii) When tissues, which have been preincubated with 2-deoxyglucose, are exposed to sugar-free solutions, intracellular free sugar decreases, but initially hexose phosphate is either unaffected, or increases [2,4].

In a number of mammalian cell lines [5,6], e.g., Novikoff rat hepatoma cells and rat B77 cells, net sugar and also nucleoside uptake is accelerated by intracellular phosphorylation, but the free sugar, or nucleosides are not accumulated above the external concentration. It is thought that transport and metabolism in these cells is linked in tandem (series); so that a high rate of substrate accumulation is maintained, by reduction of permeable substrate concentration in the cytosol below that in the external solution, by the metabolic process [5,6].

In adipocytes

Following stimulation by insulin, isolated rat adipocytes can accumulate 2-D-deoxyglucose (7 μM) by 50-fold [7]. This process is apparently dependent on phosphorylation, since saturation of the hexokinase reaction with D-glucose prevents 2-deoxyglucose accumulation; whereas 3-*O*-methylglucose, a non-phosphorylated sugar, does not inhibit uptake. 2-D-Deoxyglucose phosphate accumulates faster and to a higher concentration than free 2-deoxyglucose, indicating that phosphorylation precedes accumulation of the free sugar. Foley and Gliemann [7] have suggested that the free sugar accumulation results from its sequestration in an inaccessible compartment after dephosphorylation of the accumulation hexose phosphate. However, compartmentation is inconsistent with the finding that the entire intracellular 2-deoxyglucose pool is rapidly exchangeable with unlabelled sugar added to the external solution.

In yeasts

Whether there is accumulation of free sugar in yeasts is a matter of controversy. Earlier claims [8,9] that free sugar is accumulated in *Saccharomyces cerevisiae* were refuted when it was shown that the majority of intracellular unphosphorylated sugar was impermeant trehalose, or dideoxytrehalose [10]. Studies with petite mutant strains of yeast, which do not synthesize trehalose show no tendency to accumulate free sugar, although they accumulate hexose phosphate [11].

However, another yeast strain, *Saccharomyces fragilis* has been found to accumulate 2-deoxyglucose to higher concentrations than that in the external solution [12]. This claim remains unchallenged.

Dependence of sugar transport on metabolism is demonstrated by the finding that active galactose accumulation is observed in baker's yeast, *S. cerevisiae,* only after induction of the enzyme galactokinase. Galactokinase deficient mutants do not accumulate galactose, although passive facilitated diffusion of galactose into these cells is still observed [13]. At 0°C, in wild-type cells, sugar transport is entirely passive. At this temperature, although net flux is very much reduced, accelerated exchange and counterflow of labelled sugar are relatively rapid [14]. At higher temperatures, accelerated exchange uptake of labelled galactose into cells preincubated with high galactose concentration is only transiently observed. These findings suggest that transport and phosphorylation are separable events [13–15].

Sugar transport models

Two models are currently used to explain sugar accumulation in yeasts. (1) The Van Steveninck, or phosphotransferase system model [8,9]: sugars are actively transported into the cells by a phosphorylation step within the membrane, linked to transport. This process is similar to the bacterial phosphotransferase system (see below). In support of this model, Van Steveninck has shown that during net uptake, the specific activity of 2-deoxyglucose phosphate rises faster than that of intracellular free sugar and following inhibition with iodoacetamide, the specific activity of the 2-deoxyglucose phosphate decreases faster than that of the intracellular free sugar [8,16,17]. This has been confirmed by Franzusoff and Cirillo [18]. These results are consistent with the view that free sugar enters the cytosol mainly as a result of dephosphorylation of intracellular hexose phosphates.

Van Steveninck [9] suggests that a facilitated

transport system coexisting with an active transport system could explain the rapid tracer exchanges [13–15] into the free sugar pool.

Inhibition of the transport kinase step both increases the K_m of the transport system for sugars [16,17], and increases the exit permeability of the free sugars. These results signify that linkage of the kinase to the membrane transport system alters the nature and specificity of the active transporter. Recent genetic analysis shows that yeast strains lacking hexokinase activity have a high K_m for uptake of glucose and fructose, however, the low-K_m system of uptake could be restored by introduction of wild-type hexokinase genes [19].

(2) The alternative model for sugar transport in yeasts is that the sugar phosphorylation step takes place at an intracellular location. This is a similar model to the 'tandem' model [5,6] for transport in mammalian cells. The evidence favouring this view is that sugar transport occurs independently of accumulation, even in metabolizing cells [13–15].

Neither model accounts for the higher intracellular concentration of free sugar at stationary-state seen in *S. fragilis* [12]. In yeast, as in adipocytes [7], free sugar accumulation has been ascribed to sequestration within an intracellular compartment.

The main evidence favouring intracellular sequestration of free sugar is that following removal of the external sugar after a loading period, the decrease in intracellular free sugar concentration does not follow single-exponential kinetics [10]. Sequestration of sugar by intracellular phosphorylation is considered to result from either trapping of the sugar within the intracellular phosphate pool, or from conversion of the sugar to impermeant unphosphorylated forms, e.g. trehalose or dideoxytrehalose [10,11]; or physical trapping of free sugar within an intracellular compartment [9,20].

However, internal sequestration is difficult to reconcile with the observation [14,15], that uptake into the free sugar pool of yeasts preloaded with high concentrations, is faster than uptake into the sugar-phosphate pool.

The bacterial phosphoenolpyruvate-sugar phosphotransferase system

Sugar transport in bacteria such as *Escherichia coli, Salmonella typhimurium* and *Staphylococcus lactis* has many similarities to the above systems. Until recently, it was thought that the phosphotransferase system [21] involved obligatory coupling between the phosphorylation step within the membrane and transport (see Fig. 1). The kinetics of this model were analysed by Schachter [22].

The PTS model makes some clear predictions. Firstly, sugar uptake should be obligatorily coupled to phosphorylation, secondly, the 'stoichiometry' of sugar transport and phosphorylation should be constant; thirdly, free sugar exit cannot occur via the phosphotransferase system system, except by regeneration of phospho*enol*pyruvate from pyruvate; hence any significant free sugar exit must result from intracellular dephosphorylation of the sugars and exit via a shunt pathway.

These predictions have not been confirmed. Instead, it has been demonstrated that once introduced into the cytosol, free sugars can be phosphorylated by the phosphotransferase system and accelerated exchange exit of intracellular free sugars via the phosphotransferase system of *Staphylococcus lactis* can be stimulated by exogenous lactose. These results show that sugar transport in bacteria may also occur as a separate step from phosphorylation [23].

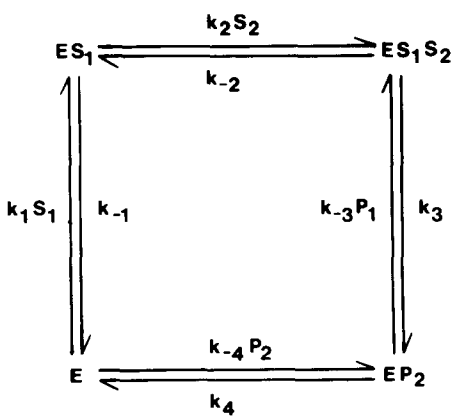

Fig. 1. Diagram showing the phosphotransferase systems, (PTS). Sugar, S_1, binds to the outside free carrier, E_1. The carrier substrate complex, $E \cdot S_1$, complexes with a phosphoryl group donor protein, S_2, to form $E \cdot S_1 \cdot S_2$; this complex undergoes a conformational change in which the sugar is transported to the inside and phosphorylated. The sugar-phosphate is shed to the inside solution leaving $E \cdot P_2$, the carrier complexed to the dephosphorylated donor protein. This dissociates to complete the carrier cycle.

General mechanism of sugar transport linked to phosphorylation

The following points can be made with regard to sugar transport linked to phosphorylation: (1) In bacteria, phosphorylating factors associated with phosphotransferase system have been shown to be tightly bound to cell membranes [24,25]. In renal tubules, sugar phosphorylation occurs specifically at the baso-lateral membranes [2,3] and asymmetric transport of 2-deoxygalactose across the winter flounder renal tubules and intestinal epithelium indicates that the kinase reaction is localized to the baso-lateral pole [26,27].

(2) A membrane associated phosphorylation reaction, for which both intracellular sugar and the sugar permeating the membrane from the outside are substrates, ensures that transport is imperfectly coupled to intracellular phosphorylation.

(3) Perfect coupling of transport and phosphorylation does not provide an explanation for the slippage between transport and phosphorylation observed in situations where there is net exit of free sugar from cells, or for net uptake of free sugar in excess of hexose phosphates.

Transport coupled to phosphorylation: microscopic model

A model which incorporates the main characteristics of the sugar transport systems outlined above is now described.

Sugar transport is considered to occur across a fixed site membrane which has identical sugar binding sites on both surfaces, the sugar crosses the membrane by successively binding to the outer and inner sites, or vice versa (Fig. 2). At the inside sites, bound sugar can also be phosphorylated via a kinase reaction using cytosolic ATP. The phosphorylated sugar and ATP are impermeant to the membrane. Permeable hexose can be regenerated within the cytosol by the action of cytosolic phosphatases.

A working physical model of a similar system, in which an anion selective membrane was coated with successive layers of hexokinase and phosphatase, has been shown to be capable of active glucose transport when ATP is present on the enzyme loaded side [28]. Similar systems have been used to demonstrate the enhanced rate of net transport of a chemical species by a membrane-coupled chemical reaction [29]. Linearized versions of these systems have been analysed by Bunow [30].

The use of network analysis to describe membrane flows coupled to chemical reactions was pioneered by Hill and Kedem [31] and has recently been usefully employed by Pietrobon and Caplan [32] to simulate non-linear chemiosmotic systems. A similar approach has been adopted here.

Carrier versus pore modes of transport

With carrier transport, it is assumed that the transported ligand and carrier traverse the membrane together as a complex, thus at any instant only one ligand can be bound to each carrier particle. Thus the maximal rate of exchange transport is functionally related to the maximal rate of carrier cycling and hence, to the maximal rate of net flux [33], i.e. it must obey the constraint that

$$R_{12} + R_{21} - R_{00} = R_{ee}$$

where $R_{12} = 1/V$(zero-*trans* 12) is the resistance to flow of carrier ligand complex from side 1 to side 2; $R_{21} = 1/V$(zero-*trans* 21) is the resistance to flow of carrier-ligand complex from side 2 to side 1; $R_{ee} = 1/V$(equilibrium exchange) is the resistance to exchange flow of the complexes and R_{00}, the resistance to flow of a complete cycle of the empty carrier, V's refer to maximal velocities. R_{00} is the resistance to free carrier movement and it is determined from the above equation.

With pore transport, the ligand is assumed to move between binding sites on either side of the membrane. Ligands may be bound simultaneously to both outside and inside sites. If the pore permits ligand exchange flux between occupied sites within the pore, then isotope exchange may occur at rates which are unrelated to the maximal rates of net flux. The total independence of the rates of exchange and net flux in the pore model can better account for the large divergences between the maximal rates of net and exchange transport which have been observed at low temperatures in both yeasts and red cell systems than carrier models do [13–15,34,35]. For this reason we prefer to use the more complex pore model to the carrier

model. However, the choice of model for permeation of sugar across the membrane is immaterial to almost all of the conclusions drawn from this paper as both pore and carrier models have identical solutions for net flux of a single ligand.

The transport cycle

The net transport process of sugar is considered as a three-state cycle (Fig. 2a), where in state N_0, the membrane is empty, i.e. no ligand is bound to either side; in state N_3, sugar is bound to the outside and in state N_1, the sugar is bound to the inside. The states are interconnected by symmetrical pseudo-first-order, or first-order forward and backward rate constants [31], depicted here as a single line. The constants determine the transition rates between the states (see Appendix).

Each cycle resulting in net transport begins and ends in the empty state, N_0. Thus the following sequence occurs during net inflow $N_0 \rightarrow N_3 \rightarrow N_1 \rightarrow N_0$ and the reverse for exit (Fig. 2a). At equilibrium, with equal concentrations of sugar in the bathing solutions on either side, the flux from outside to inside equals the flux from inside to outside and there is an equal probability of the membrane being in state N_3 and N_1.

Because the empty state of the membrane, N_0, is a single state, the side of the membrane to which a particular ligand is bound, or lost is not immediately obvious. This additional information can be obtained from the pictograms beside each node in the network, which represent the position and type of ligand(s) bound.

The phosphorylation reaction cycle

An ordered kinase reaction is assumed to transfer a phosphoryl group from ATP, present in the cytosol, to sugar bound to the inner sites, state N_1, to form sugar phosphate and ADP on the inner surface, state N_2. Then ADP and the impermeant sugar phosphate dissociate into the inner solution to reform the empty state, N_0. Thus forward progress of the phosphorylation cycle involves the sequence of transitions $N_0 \rightarrow N_1 \rightarrow N_2 \rightarrow N_0$ at the inner site. This simplified version of network, where the steps involving nucleotides are condensed, is shown in Fig. 2b, the full scheme is shown in Fig. 2c.

Incorporation of the thermodynamic potential of the reaction into the network

If cytosolic [ATP], [ADP], [free sugar] and [hexose phosphate] are near to equilibrium with the bound forms of these ligands, then a forward to backward flux ratio of transitions of the phosphorylation cycle, $N_1 \rightarrow N_2 / N_2 \rightarrow N_1$ is determined by the driving force, or Gibb's free energy, ΔG_h, of the hexokinase reaction

$$\text{2-deoxyglucose} + \text{ATP} \rightleftharpoons \text{2-deoxyglucose 6-phosphate} + \text{ADP} \tag{1}$$

where

$$-\Delta G_h = -\Delta G_h^0 + RT \ln\left\{\frac{([\text{ATP}]\cdot[\text{2-deoxyglucose}])}{([\text{ADP}]\cdot[\text{2-deoxyglucose 6-phosphate}])}\right\} \tag{2}$$

and ΔG_h^0 is the standard free energy of the hexokinase reaction. $\Delta G_h^0 = -19$ kJ/mol [36].

Within the physiological range of concentrations of ATP (5–10 mM) and ADP (20–100 μM), free sugar (1–5 mM) and hexose-phosphate (10–30 mM) the Gibb's free energy of the hexokinase reaction is in the range -25 to -30 kJ/mol, i.e.

$$N_1 \rightarrow N_2 / N_2 \rightarrow N_1 = \exp(-\Delta G_h / RT)) \tag{3}$$

Hence from Eqn. 2

$$N_2 \rightarrow N_2 / N_2 \rightarrow N_1 = \exp(-\Delta G_h^0 / RT) \cdot ([\text{ATP}]\cdot[\text{sugar}]) / ([\text{ADP}]\cdot[\text{hexose phosphate}]) \tag{4}$$

is in the range 22 000–170 000. At equilibrium, the ratio is 1.

The component due to standard free energy ΔG_h^0 of the hexokinase reaction is constant, independent of concentrations of the reactants, or products. This factor can be incorporated into the network by making the microscopic rate constants of the hexokinase reaction asymmetric. Thus when equimolar concentrations of the components of the hexokinase reaction are present, the ratio of forward rate, s, to backward rate, p, of the phosphorylation cycle (see Fig. 2g) is

$$s/p = N_1 \rightarrow N_2 / N_2 \rightarrow N_1 = \exp(-\Delta G_h^0 / RT) = 2600 \tag{5}$$

A single constant, E, may be substituted for

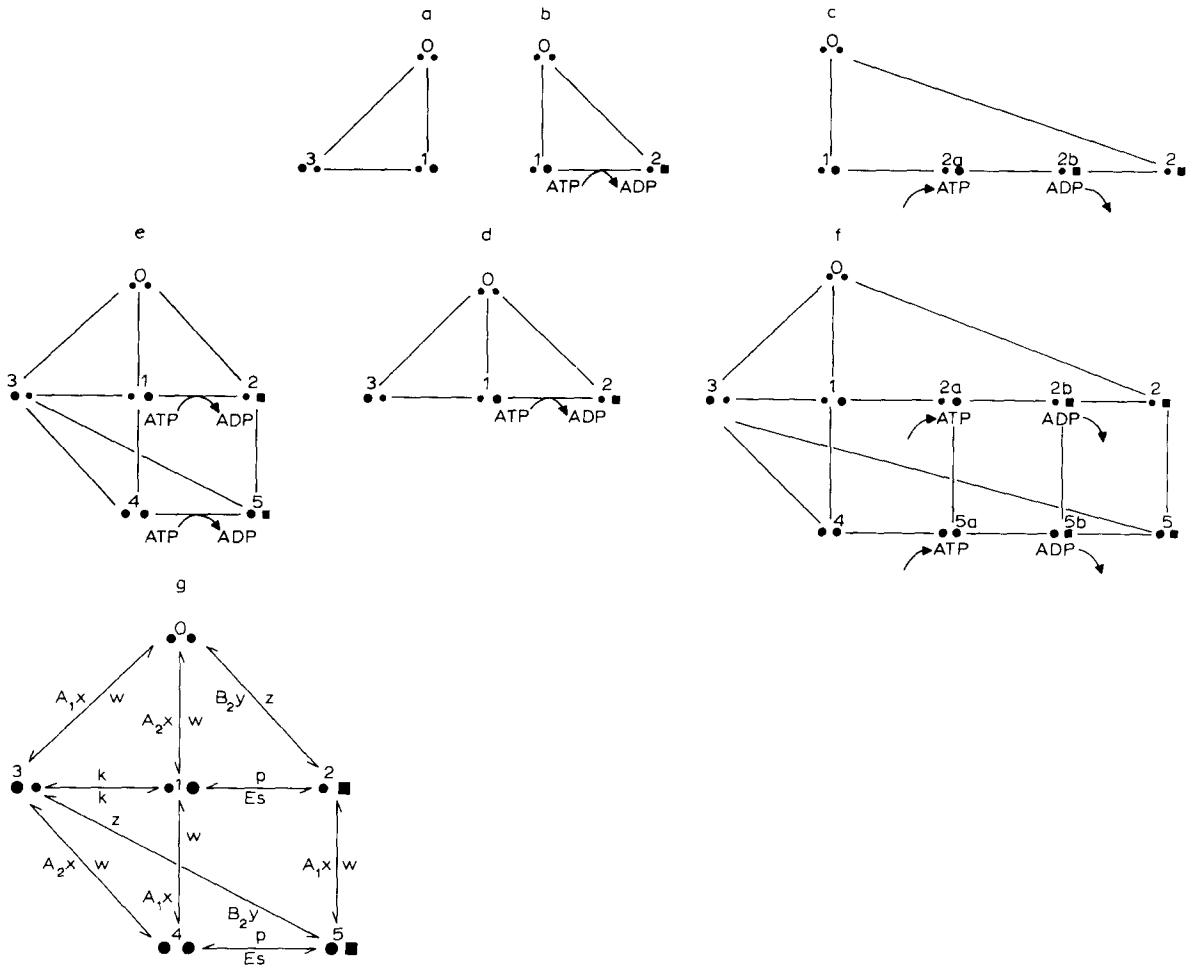

Fig. 2.(a) The transport cycle. The two dots in N_0 represent outside (left) and inside (right) vacant sites. Sugar A_1 (filled circles), from outside binds to outside sites to form state N_3; sugar from inside, A_2, binds to inside sites to form state N_1. The lines between the states represent the bidirectional rates of transition connecting adjacent states.

(b). The abbreviated phosphorylation cycle. Sugar bound to inside sites (filled circles on right sites), can be transformed to hexose phosphate bound to the inner sites, state N_2 (filled squares), by the action of hexokinase in the presence of ATP (T_2). The reverse cycle occurs when hexose phosphate (B_2), and ADP (D_2), from the inside solution bind to the inside sites and are transformed to sugar, N_1 and ATP.

(c) The extended form of the phosphorylation cycle. ATP binds to internal sites occupied by sugar, state N_{2a}. The sugar- ATP complex is transformed to hexose-phosphate-ADP complex, state N_{2b}, before being transformed to bound hexose phosphate, N_2. These transformation steps are reversible. The advantage of Fig. 2c over Fig. 2b is that [ATP] and [ADP] are independent and each ligand has its own separate affinity for the binding sites (here K_d values for ATP and ADP are 1 mM).

(d) The combined transport and phosphorylation cycles. Impermeant hexose phosphate has no direct access to the external site.

(e) This figure includes the additional doubly occupied states. State N_4 has sugar bound both to inside and outside sites. State N_5 has sugar bound to the outside and hexose phosphate bound inside. The hexokinase action transforms sugar bound at the inner sites, either in the single-ligand state, N_1, or double-ligand form, state N_4 to hexose phosphate in state N_2, or N_5, respectively.

(f) This figure is the extended 10 state version of Fig. 2e, combining the double-ligand states, shown in (e), with the extended phosphorylation cycle, as shown in (c). This is the form used to simulate the results shown in Figs. 4–6.

(g) A diagram showing the separate rate constants for the 6-state network of a membrane separating solutions 1 and 2. The association rates are the product of ligand concentration and the second-order association constant. The concentrations of sugar isotopes are represented by the following codes: A_1, the concentration of free sugar in the external solution 1; A_2, the free sugar concentration in the cytosol 2; B_2, is the concentration of hexose phosphate in the cytosolic solution. The rates of ligand association with vacant sites are considered to be pseudo-first-order constants, which are the products of ligand concentration with the appropriate the second-order association constants, x and y; e.g. (A_1 or A_2)$\cdot x$ and $B_2 \cdot y$. The rates of dissociation of sugar and hexose phosphate from sites, w and z, respectively, are first-order constants; hence the dissociation constant of free sugar is w/x and that of hexose phosphate is y/z. s is the forward rate constant of the hexokinase reaction and p, the reverse rate. k is the rate of intersite mobility of sugar. E is equivalent to the ratio [ATP]/[ADP]. The pictograms beside each node are shown in Fig. 2e.

[ATP]/[ADP] in the right hand side of Eqn. 4.

Combination of Eqns. 4 and 5 gives the following simple expression for the ratio of forward to reverse rate of the phosphorylation cycle.

$$N_1 \rightarrow N_2 / N_2 \rightarrow N_1 = (E \cdot s \cdot [\text{sugar}])/(p \cdot [\text{hexose phosphate}]) \quad (6)$$

The force-flow relationships of transport coupled to the abbreviated phosphorylation cycle, Fig. 2d, are qualitatively similar to the linear range of operation of the full phosphorylation cycle (Fig. 2f). The reduced system is useful, as it permits a simple analytical solution to be obtained for the conditions giving stationary state distributions of free sugar. It also reduces the minimal number of states required to simulate isotope exchange in a pore to 15 (see below).

The assumption that the effect exerted by ATP and ADP on the ratio of forward to backward flux within the hexokinase reaction is linearly related to E (see Eqn. 6) is only justified over a limited range. The full 10-state network solution (Fig. 2f) does not require the assumption that the free and bound components of the hexokinase reaction are close to equilibrium. Acceleration of sugar transport by [ATP]-dependent stimulation of the hexokinase reaction is a saturable function of [ATP] (see Figs. 4(d,e)). Similar observations have been made previously by Zoratti, Pietrobon and Azzone [37] and Pietrobon and Caplan for chemiosmotic systems [32].

Irreversible processes in loosely coupled networks

Coupling between any two cyclic processes may occur when they have one or more steps in common, as in the examples shown in Figs. 2 and 3 [31,38–41]. Loose coupling can only occur if the components of each cycle can flow independently as well as in coupled modes.

Independence of the separate flows of components across the network is ensured by having one cycle per component, where the component entry to and exit from the network is via the empty state, N_0. Entry, or exit of ligands at any other point in the network, although permitted, implies that the flow from that step is entirely dependent on a preexisting state, determined by interaction with another ligand, e.g., the exchange flux mode (Fig. 3).

In the models illustrated in Figs. 2 and 3, each cycle can operate separately, or together via the shared, or separate paths; hence, there is always some leakage, or 'slippage' of cycling components via the alternative shunting branches. This ensures that the coupling process is irreversible; i.e. the efficiency of coupling is less than 100%. In these respects the models in Fig. 2 differ from the reversible type illustrated in Fig. 1.

Rectification and slippage

The transport and phosphorylation cycle may be combined as follows: sugar outside the membrane binds to a vacant external site, ($N_0 \rightarrow N_3$), crosses the membrane ($N_3 \rightarrow N_1$), is phosphorylated inside the membrane ($N_1 \rightarrow N_2$), and released as sugar phosphate inside ($N_2 \rightarrow N_0$). Influx of sugar is thereby accelerated because the kinase action depletes sugar bound to the inside sites and the product of the phosphorylation reaction, hexose phosphate, dissociates only into the intracellular solution.

When an inwardly directed concentration difference of free sugar exists, net inflow of free sugar via the cycle $N_0 \rightarrow N_3 \rightarrow N_1 \rightarrow N_0$ may be observed in addition to inflow via the transport and phosphorylation cycle, $N_0 \rightarrow N_3 \rightarrow N_1 \rightarrow N_2 \rightarrow N_0$. This is an example of slippage. Passive inflow of free sugar is reduced by the phosphorylation reaction, which diverts bound-sugar in state N_1 into the phosphorylation cycle. As sugar bound to the membrane from the inside solution may also be phosphorylated via a second possible phosphorylation cycle, $N_0 \rightarrow N_1 \rightarrow N_2 \rightarrow N_0$ (Fig. 2e), free sugar outflow via the cycle $N_0 \rightarrow N_1 \rightarrow N_3 \rightarrow N_0$ will be retarded. Net outflow of free sugar via the transport cycle commences only when the free sugar concentration inside rises to a level where the fractional probability of the membrane state N_1 exceeds state N_3. Flow via this cycle is a second example of slippage between the transport and phosphorylation reactions.

Thus the phosphorylation reaction changes the symmetrical passive transport system into an asymmetric system. This acts as a rectifier to the flow of free sugar. If free sugar is generated within the cytosol from hexose phosphate via a futile

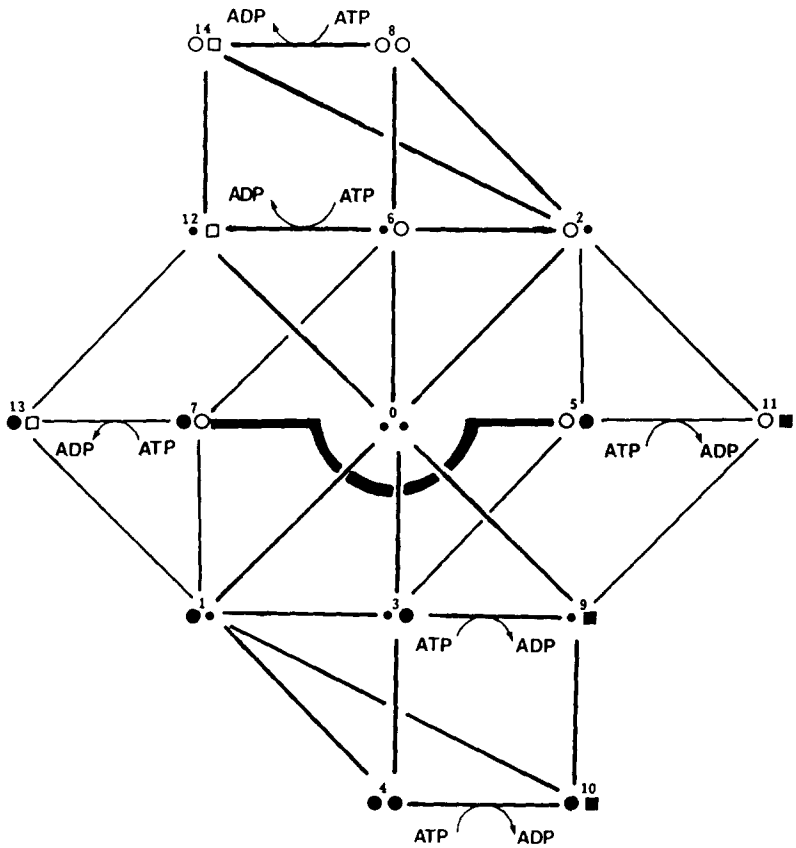

Fig. 3. The network of states required for transport and exchange of two sugar isotopes, A and C (open and filled circles), with phosphorylation of both sugar isotopes at the inner sites to form hexose phosphate, B_2 and D_2 (open and filled squares). The basis of this network is a duplicated form of network shown in Fig. 2e. The empty state N_0 is common to both isotopes, there is also provision for binding of isotope mixtures. Transformations between the forms N_5 and N_7 permit exchange of mobile bound sugar between the inside and outside sites in the absence of net flux.

phosphatase cycle, the rectifying system will be capable of maintaining large stationary state concentration differences of free sugar across the membrane.

Network representation of the pore model

Network representation of the pore transport model requires two doubly occupied states, in addition to the single ligand states shown in Fig. 2d (see Fig. 2e). The cycles which start and finish at state N_0 and contain either of the doubly occupied states, N_4 and N_5, do not permit net transport, hence act as retardants to flow, e.g., $N_0 \rightarrow N_3 \rightarrow N_4 \rightarrow N_1 \rightarrow N_0$, or $N_0 \rightarrow N_3 \rightarrow N_5 \rightarrow N_2 \rightarrow N_0$. Thus, hexose phosphate prevents free sugar transport by reducing the probability of empty sites at the inner surface. Similarly, sugar bound to the innersites prevents net uptake from the outside and vice versa.

Analytical solution for the zero-flow stationary state

When net flow of sugar across the pore transport system is zero, the probability of occurrence of state N_1 and state N_3 are equal (Figs. 2e and 2g). Using this constraint and the set of five independent equations shown in matrix form in Table Ia, it is possible to obtain a simple analytical solution for the stationary state distribution of free sugar across the transporter $[A_2]/[A_1]$ (A_2/A_1).

The appropriate solution is

$$\frac{[A_2]}{[A_1]} = \frac{E \cdot s \cdot z}{w \cdot (z+p)} - \frac{[B_2] \cdot y \cdot p}{[A_1] \cdot x \cdot (z+p)} + 1 \qquad (7)$$

$[A_1]$ and $[A_2]$ refer to the sugar concentrations in the outer and inner bathing solutions, respectively, $[B_2]$ (B_2) is the intracellular hexose phosphate concentration. s and p are the forward and reverse rates of the hexokinase reaction, the ratio of these constants, s/p is determined by $\exp\{-\Delta G_h^0/RT\}$; x and y are the second-order association rates of free sugar and hexose phosphate, respectively for the sugar binding sites; w and z are the first-order dissociation rates of free sugar and hexose phosphate, respectively, from the sites and E is [ATP]/[ADP] (see Eqn. 5).

When the rate of the hexokinase reaction on the membrane is zero, $s = p = 0$, and hence the distribution ratio of free sugar = 1.

In the physiological concentration range of components of the hexokinase reaction, the reverse rate, p, is approx. 0.005% of the forward rate, s [6]. Hence, when the concentration of intracellular hexose phosphate, $[B_2]$ is 'low', Eqn. 7 simplifies to

$$\frac{A_2}{A_1} \approx \frac{E \cdot s}{w} + 1 \qquad (8)$$

Eqn. 8 indicates that the steady-state distribution ratio of free sugar is determined mainly by:

(a) $E \cdot s$ the factor by which the forward rate of the hexokinase reaction is accelerated by the free energy of the hexokinase reaction, and

(b) the ratio of the forward rate of the hexokinase reaction on the membrane, $E \cdot s$, to the dissociation rate of free sugar for the binding sites, w (see Fig. 2g).

It should be emphasized that this stationary state accumulation of free sugar depends entirely on the continuous cycling of the hexokinase reaction and hence on continuous dissipation of some energy resource external to the coupling process – namely, a supply of ATP from metabolism.

Numerical solutions to sugar flux equations

In the next section, the effects of varying [ATP] and [ADP] are shown, hence the ten-state model (Fig. 2f) is required to simulate these effects as the six state model uses only the ratio [ATP]/[ADP] as a force variable.

Effects of varying ATP and intracellular free sugar on the rate of total sugar uptake

The effects of varying internal cytosolic [free sugar] at different concentrations of ATP on the steady-state rate of total net sugar uptake are shown in Fig. 4a. Total net sugar uptake refers to net uptake of sugar from the external solution into the cytosolic pools of both free sugar and hexose phosphate. Free sugar loss, refers to loss from the cytosolic free sugar pool into the external solution. For convenience, all the fluxes are normalized to the area of membrane surrounding 1 cm^3 of cell volume, assumed to be unit area. The steady-state rates are obtained at fixed concentrations of all reactants and products.

In the absence of a driving force for the hexokinase reaction, i.e. at low [ATP] (5 μM), sugar uptake depends entirely on passive facilitated transport across the pore. The rate of net sugar uptake falls to zero as the concentration of intracellular free sugar approaches the external concentration. Raising the cytosolic [free sugar] above the external concentration results in the net outflow, represented as a negative flux falling below the dotted line. When [ATP] is raised, the rate of total net sugar uptake is increased. This increased uptake is observed even when free sugar is absent from the cytosol (see below). Raising cytosolic [free sugar] still reduces net inflow, however, now the cytosolic [free sugar] must be raised substantially above the external [sugar] before net exit is observed, i.e., the apparent K_i for trans inhibition of total net sugar uptake by cytosolic [sugar] is raised when [ATP] is increased.

Effect of ATP on total net sugar uptake and on free-sugar loss from cells

Uptake

The effect of changing [ATP] with fixed [ADP], [hexose phosphate] and both intracellular [free sugar] and extracellular [sugar] held equal to 1 mM is shown in Fig. 4b. With [ATP] at 1 μM, no net flow of free sugar occurs. With logarithmic increases in [ATP], there is a saturable increase in

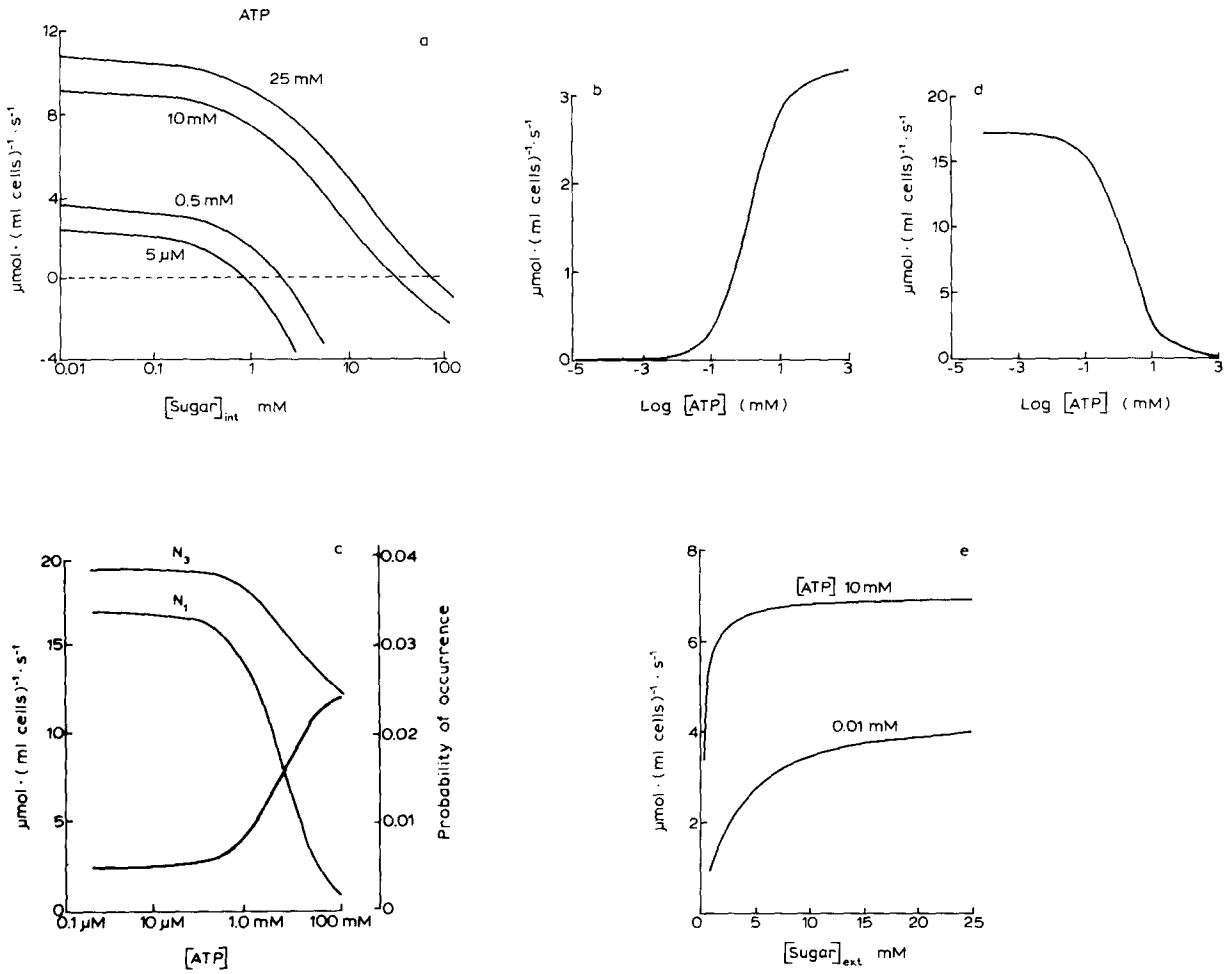

Figs. 4–6. The following constants are common to all Figs. 4–6, unless otherwise states for network key (see Fig. 2g).

First-order constants:

k, sugar intersite mobility constant, determining $N_1 \rightarrow N_3$ or $N_3 \rightarrow N_1$ transition rates; $k = 500\ s^{-1}$.

w, the sugar dissociation rate, determining $N_1 \rightarrow N_0$, etc.; $w = 25\ s^{-1}$.

z, the hexose-phosphate dissociation rate determining $N_2 \rightarrow N_0$, etc., $z = 100\ s^{-1}$.

s, sugar phosphorylation rate, determining $N_1 \rightarrow N_2$ transformation; $s = 130\ s^{-1}$.

$p = 0.05\ s^{-1}$, the reverse rate of phosphorylation determining $N_2 \rightarrow N_1$ transitions, hence, $s/p = 2600$.

The second-order rates:

x, the rate association of free-sugar for vacant site; $x = 100\ mM^{-1} \cdot s^{-1}$.

y, the association rate of hexose phosphate for vacant sites; $y = 100\ mM^{-1} \cdot s^{-1}$.

The dissociation constant of sugar for sites, $K_d = w/x = 0.25$ mM.

The dissociation constant of hexose phosphate for sites, $K_d = z/y = 1$ mM.

In the 10 state network (Fig. 2f), where [ATP] and [ADP] are independent variables, the first-order dissociation rates of both ATP and ADP are $100\ s^{-1}$ and at 1 mM the pseudo-first-order association rates of ATP and ADP are $100\ s^{-1}$, hence the theoretical K_d values for ATP and ADP are 1 mM.

Cytosolic concentrations of ADP 20 μM and ATP 10 mM, unless stated otherwise. The term 'total net sugar uptake' is defined as the steady-state rate of uptake of sugar from the external solution into both the intracellular free sugar pool and hexose phosphate pool. Uptakes are expressed as if they were into 1 ml of cell water. The area of membrane surrounding this volume is normalized to unit area. Exit of free sugar is the rate of loss of free sugar from the cell. Both total net sugar uptake and net free sugar loss are expressed across the same unit area of membrane.

total net sugar inflow (the apparent K_m for ATP-dependent increase in net sugar uptake is 1.2 mM, the theoretical $K_m = 1$ mM). The saturable effect of raising [ATP] on sugar flows is due to the saturable increase in bound [ATP] with changes in intracellular [ATP] (Fig. 5b).

The effect of altering [ATP] and hence the rate of phosphorylation on total net influx, when intracellular [free sugar] is maintained at zero is shown in Fig. 4c. Additionally, the proportion of membrane states which favour inflow, state N_3 and outflow, state N_1, (see Figs. 2d and 2e) are shown: in the absence of cytosolic sugar and any hexokinase activity, the internal sites will be occupied by mobile sugar to an extent which depends on the relative rates of sugar permeation through the membrane from the external sites and dissociation of sugar from the internal sites into the cytosol. Hexokinase activity at the inner sites accelerates net uptake by decreasing the probability of finding mobile sugar ligand bound to the inner sites, state N_1. This increases both the maximal rate of a net sugar uptake, V_m and reduces the apparent K_m for net sugar uptake (see below).

Exit

When intracellular free sugar is present initially at 47 mM and extracellular [sugar] at 0.1 mM, there is net exit of sugar via the cycle $N_0 \rightarrow N_1 \rightarrow N_3 \rightarrow N_0$ (Fig. 2e). This process is opposed by the phosphorylation cycle, $N_0 \rightarrow N_1 \rightarrow N_2 \rightarrow N_0$. Raising [ATP] increases flow via the phosphorylation cycle at the expense of the transport cycle, thereby reducing net exit. Fig. 4d shows that raising [ATP] decreases the rate of free sugar exit ($K_i = 1.2$ mM). This demonstrates that the phosphorylation reaction at the inner binding sites can retard net sugar exit without any requirement for intracellular sequestration.

Effects of ATP on K_m and V_m of net sugar uptake

The effects of varying external sugar concentration, with high and low concentrations of cytosolic ATP, on the estimated 'initial' rates of total net sugar uptake (free + phosphorylated sugar), are shown in Fig. 4e. These rates were obtained by integrating the rates of total sugar accumulation into the free sugar and hexose-phosphate pool over the first 0.25 s of uptake. The integral takes account of the rate of conversion of cytosolic hexose phosphate to free sugar resulting from the phosphatase reaction within the cytosol. It is assumed that the only time-dependent variables are cytosolic [free sugar] and [hexose phosphate]; [ATP] and [ADP] remain constant. It is also assumed that the cell volume remains unchanged.

Increasing cytosolic [ATP] from 0.01 mM to 10 mM, decreases the apparent K_m for 'zero-*trans*' total net sugar uptake from 3.2 mM, (theoretical value 0.25 mM) to 0.25 mM and also increases the

---

Fig. 4. (a) The effects of varying intracellular [free sugar] from a negligible concentration to 100 mM and [ATP] on the rate of total net sugar uptake from external solutions containing 1 mM sugar. The separate lines are with [ATP] fixed at: 25 mM, 10 mM, 0.5 mM, or 5 μM: intracellular [hexose phosphate] = 17 mM and [ADP] = 20 μM. The intercept on the dotted line is the intracellular [sugar] required to reduce total net inflow to zero. This is 70 mM, 24 mM, 2.4 mM and 1.1 mM with the decreasing concentrations of ATP.
(b) The effect of changing [ATP] on the rate of total net sugar uptake. The following remain constant: [ADP] = 20 μM, extracellular and intracellular [free sugar] = 1 mM and [hexose phosphate] = 17 mM. The apparent K_m of ATP-dependent activiation of sugar flux = 1.2 mM (theoretical, K_d for ATP = 1 mM).
(c) The effect of varying [ATP] on the rate of total net uptake of sugar from an extracellular solution containing 1 mM sugar (thick line), into cells with cytosolic free sugar absent, instead of 1 mM, as in Fig. 4b; [hexose phosphate] = 17 mM, [ADP] = 20 μM. The thin lines represent the fractional probabilities of occurrence of the membrane states, N_3 and N_1 (see Figs. 2d–f), the states required to generate net sugar inflow and outflow, respectively.
(d) The effect of changing [ATP] on the initial rate of net exit of free sugar, from cells containing 47 mM free sugar into an external solution containing 0.1 mM sugar; cytosolic [hexose phosphate] = 17 mM, [ADP] = 20 μM.
(e) The effect of varying external [sugar] on total net sugar uptake. The cells contain either low [ATP] (0.01 mM), or high [ATP] (10 mM). The rates of uptake are obtained from the accumulation of sugar and hexose phosphate in 0.25 s, obtained by integration. The initial intracellular concentrations of both free-sugar and hexose-phosphate are zero. The apparent K_m and V_m for net uptake are estimated by non-linear least-squares regression analysis. With 0.01 mM ATP, the K_m for total net uptake of sugar is 3.2 mM and the $V_m = 4.5$ μmol·(ml cells)$^{-1}$·s^{-1}. With 10 mM ATP, the K_m for total net uptake is 0.25 mM and $V_m = 6.5$ μmol·(ml cells)$^{-1}$·s^{-1}. The theoretical dissociation constant, K_d, of sugar for the binding sites is $w/x = 0.25$ mM.

apparent V_m. These effects are caused by the decreased proportion of inside sites occupied by sugar when the hexokinase reaction rate increases (see Fig. 4c).

The results shown in Fig. 4e, suggest a possible explanation for the rise in apparent K_m for total sugar uptake into inhibited yeasts cells [16,17] or into hexokinase deficient yeasts [19], namely: more of the inside sites are occupied by sugar in energy depleted, or hexokinase-deficient cells than in controls. This causes *trans*, or 'product' inhibition of net influx and thereby increases the apparent K_m and reduces the apparent V_m of influx.

Accelerated uptake of non-metabolized, but transported sugars can also be explained in terms of this model, if raised metabolic activity reduces the concentration of non-transported intracellular ligands which would otherwise retard sugar uptake by binding to internal sites [19] (see Fig. 5c).

The effects of altering the dissociation rate of sugar for the binding site on total net sugar uptake

Fig. 5a shows a plot of the steady-state total net sugar uptake (positive), or net free sugar efflux (negative), as a function of intracellular free sugar concentration, log(mM). Net flow is zero at the intersection with the dotted line. Intracellular concentrations of hexose phosphate, ATP and ADP are held constant (see legend).

The lines show the effect of altering both w, the dissociation rate and x, the association rate of sugar from and to the membrane binding sites (see Fig. 2g) whilst the dissociation constant of sugar is held constant ($K_d = w/x = 0.25$ mM). Fig. 5a illustrates that an increase in the rate of sugar dissociation, w, relative to the rate of phosphorylation of the bound sugar, decreases both the stationary state distribution ratio of free sugar and the net rate of sugar accumulation, (see Eqns. 6 and 7). Thus, a sugar with a high affinity for the binding site, e.g., 2-deoxyglucose, is likely to be accumulated to a greater extent than sugars with lower affinity, e.g. D-galactose [1–3].

The effects of altering the rate constants of the membrane associated hexokinase reaction on net sugar uptake

In Fig. 5b, the steady-state rate of total net sugar uptake is plotted as a function of intracellular [free sugar] at three different forward rates of phosphorylation, s, of the sugar bound to the inner sites (see Fig. 2g). The forward to backward rate ratio of the hexokinase reaction is held constant ($s/p = 2600$). When s is increased, both the rate of total net sugar uptake and the stationary state distribution ratio of free sugar are increased (Fig. 5b).

Figs. 5a and 5b illustrate that both the stationary state distribution of free sugar and the rate of total net uptake as predicted by Eqns. 7 and 8, are dependent on the ratio of hexokinase rate at the inner sites to dissociation rate of free sugar.

The effects of varying the intracellular concentrations of hexose phosphate and free sugar on total net sugar uptake

The effects of three different internal concentrations of hexose phosphate (theoretical K_d for the transport sites is 1 mM) on the steady-state total net sugar fluxes from a fixed external sugar concentration (1 mM) into cytosol containing a range of intracellular [free sugar] are shown in Fig. 5c. Cytosolic [ATP] and [ADP] are held constant.

Raised concentrations of hexose phosphate decrease the rate of net sugar accumulation, but have only a small effect on the stationary-state accumulation ratio of free sugar, as seen from the intersection of the lines at zero flow.

The small effect of [hexose phosphate] on the stationary state distribution of free sugar is consistent with predictions of Eqn. 7.

An impermeant competitive inhibitor could only exert a significant effect on the stationary state distribution ratio of free sugar if its affinity for the sugar transport sites were at least two orders of magnitude greater than that of the transported sugar.

Simulation of the time-course of net uptake of sugar at high and low rates of cytosolic phosphatase activity

In Figs. 6a, 6b and 6c, the time-courses of the changing concentrations of free sugar and hexose phosphate within the cytosol are simulated by numerical integration of the stationary state rates. It is assumed that the only system variables are the cytosolic sugar and hexose phosphate concentrations; the external sugar concentration is

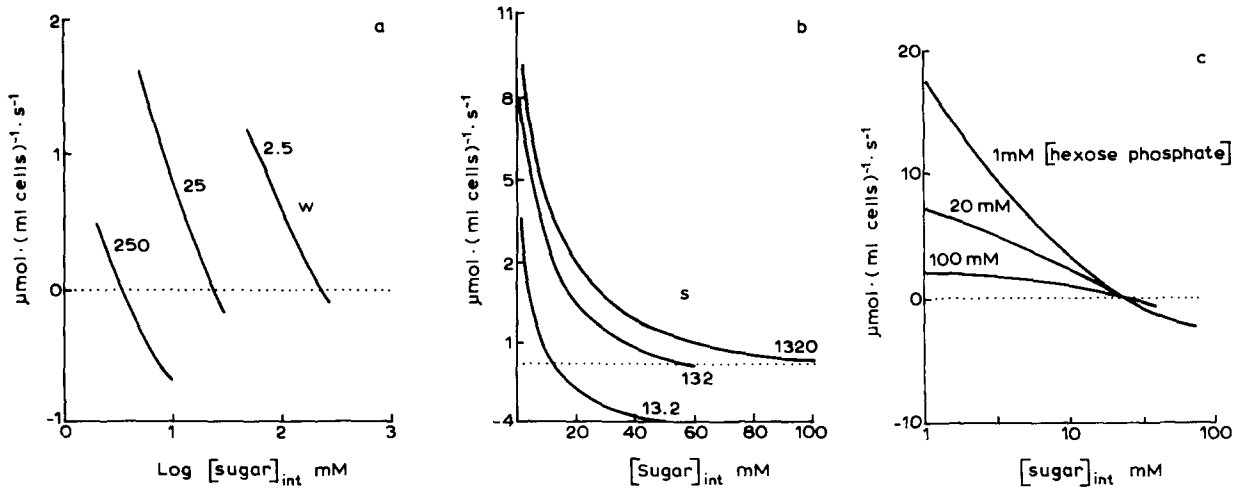

Fig. 5. (a) The effects of varying intracellular [free-sugar] on the rate of total net sugar uptake from external solutions containing 1 mM free sugar, at three different dissociation rates, w, of free sugar for the binding sites, i.e., $w = 250\ s^{-1}$, $25\ s^{-1}$, and $2.5\ s^{-1}$. x the association constant of sugar for vacant sites is also changed from 1000 $mM^{-1} \cdot s^{-1}$, to 100 $mM \cdot s^{-1}$ and 10 $mM^{-1} \cdot s^{-1}$, respectively; hence the $K_d = w/x$ of sugar for the sites is maintained constant at 0.25 mM; [hexose phosphate] = 17 mM; [ATP] = 10 mM and [ADP] = 20 μM.

(b) The effects of varying intracellular [free sugar] on the rate of total net sugar uptake from an external sugar containing 1 mM free sugar, at three different rates of phosphorylation, i.e., $s = 1300\ s^{-1}$, $130\ s^{-1}$ and $13\ s^{-1}$. The reverse rate is also changed from 0.5 s^{-1}, to 0.05 s^{-1} and 0.005 s^{-1}, respectively, so that the ratio $s/p = \exp(-\Delta G_h^0/RT)$ at equimolar concentrations of ATP, ADP, hexose phosphate and free sugar is held constant at 2600.

(c) The effects of varying intracellular [free sugar] on the rate of total net sugar uptake from an external solution containing 1 mM sugar, at intracellular [hexose phosphate] = 1 mM, 20 mM, or 100 mM. Cytosolic [ATP] = 10 mM and [ADP] = 20 μM.

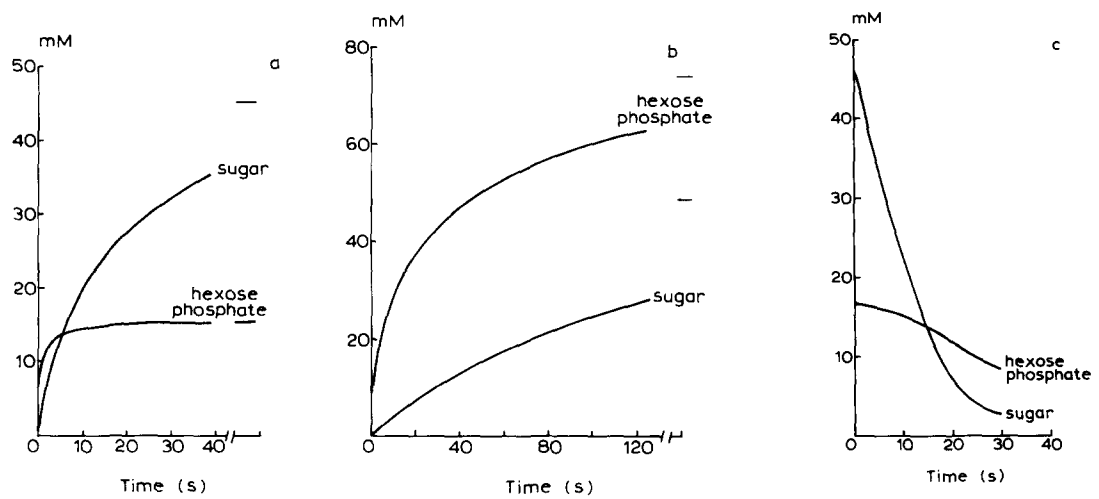

Fig. 6. The simulated time-course of accumulation of free sugar from an external sugar concentration of 2 mM. In Fig. 6a there is a high intracellular phosphatase activity ($1.5\ s^{-1}$). In Fig. 6b, there is a low intracellular phosphatase activity ($0.25\ s^{-1}$). In both 6a and 6b, the stationary state concentration of free sugar is 47 mM, the hexokinase rate is also the same in both 6a and 6b.

(c) The time-course of loss of intracellular [free sugar], initial concentration 47 mM into an external solution of 0.1 mM. The initial hexose phosphate concentration is 17 mM. The intracellular phosphatase activity is high ($1.5\ s^{-1}$), as in Fig. 6a.

fixed at 2 mM and the cytosolic [ATP] and [ADP] remain constant. The rate of conversion of hexose phosphate to free sugar by cytosolic phosphatase is assumed to be directly proportional to cytosolic [hexose phospahte]. The cytosolic phosphatase rate is six times faster in Fig. 6a than in Fig. 6b, otherwise all other parameters and variables are the same.

Initially, free sugar and hexose phosphate are absent from the cytosol, so passive uptake of free sugar occurs in parallel with its conversion to hexose phosphate and subsequent release to the cytosol. Hence, total net sugar uptake, (free sugar + hexose phosphate) initially exceeds hexose-phosphate accumulation. This is also the pattern predicted by the tandem process of transport and intracellular phosphorylation [5,6].

Total sugar accumulation quickly slows as free sugar and hexose phosphate accumulate. If there is a high activity of cytosolic phosphatase relative to the total cell hexokinase activity, then free sugar may appear to accumulate more rapidly and to a greater extent than hexose phosphate (Fig. 6a), as observed in hamster renal epithelium [4] and occasionally in yeasts [18]. This is also similar to the kinetic behaviour predicted by the tandem model [5,6].

The absence of correlation between net sugar exit and phosphorylation rate

In Fig. 6c the intracellular concentrations of free sugar and hexose phosphate are set initially at the levels required for the zero-flow stationary state with 2 mM sugar present in the external solution, as shown in Fig. 6a. The hexokinase and phosphatase activities are also the same as those in Fig. 6a. At zero-time the external sugar concentration is reduced from 2 mM to 0.1 mM and net free sugar exit begins immediately, hence intracellular [free sugar] decreases. However, no matching change occurs with intracellular [hexose phosphate], because the hexokinase still generates hexose phosphate from the sugar binding to the inner sites from the cytosol source.

In real systems cytosolic hexokinase action could also play a part in maintaining hexose phosphate levels following reduction in external sugar concentration: however, this effect is not simulated here.

Because it was previously assumed that transport and phosphorylation in epithelia and yeasts must either be tightly coupled, or uncoupled, [3,4,10], the apparent dissociation between free sugar flux and phosphorylation rate cast doubt on the view that transport and accumulation of free sugar are coupled. In the situation displayed in Fig. 6c, the absence of correlation between net exit of sugar and net phosphorylation is an example of slippage in a loosely coupled system.

Exchange

A network which simulates independent net flux across a pore of two mobile isotopically labelled sugars, A and C, with identical affinities for the binding sites ($K_d = 0.25$ mM) and also simultaneous exchange flux and phosphorylation by hexokinase of the two isotopes at the inner site to form isotopic forms of hexose phosphate, B and D ($K_d = 1$ mM), from A and C, respectively, requires a minimum of 15 states. The network shown in Fig. 3 is similar to that shown in Fig. 2e, but enlarged to include the states where the network is occupied by the other ligand alone and the extra double-ligand states, which represent all the possible states where isotope pairs are simultaneously bound to inside (side 2), and outside (side 1), i.e., A_1A_2; A_1B_2; A_1C_2 and A_1D_2, also C_1A_2; C_1B_2; C_1C_2 and C_1D_2. The possible interchange between the two states N_5 and N_7 (Fig. 3), which bind mixed pairs of mobile ligands, A_1C_2; C_2A_1, provides the basis for exchange flux.

Although the total number of rate constants required for pore exchange is the same as for a symmetrical mobile carrier, pore exchange imposes a large increase in network complexity, thereby making analytical solution impractical. However, solutions to the 14 independent simultaneous equations for the pore model can be obtained by iterative matrix methods (see Appendix).

Simulation of exchange

The effects of increasing the rate of phosphorylation of sugar ligand bound to the inner surface on the initial rates of unidirectional and net fluxes of sugar are shown in Figs. 7a and 7b. Initially, only one of the isotope forms is present in the cytosolic pool, free sugar, C_2, and hexose phos-

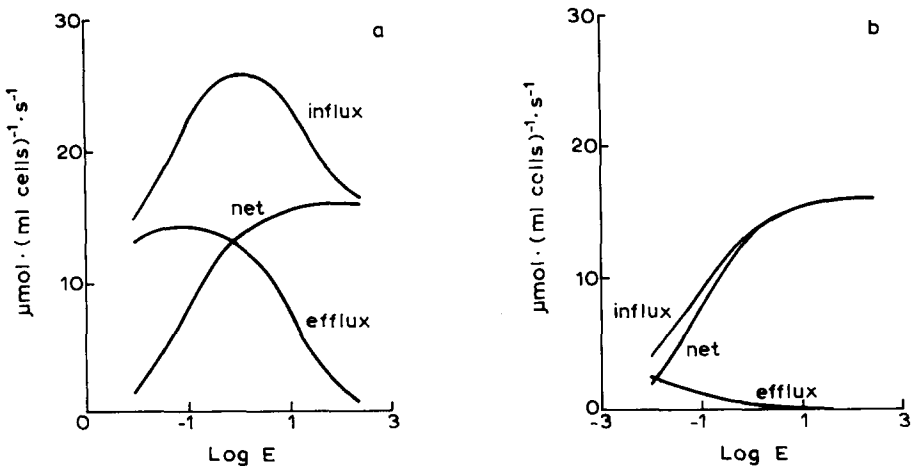

Fig. 7. (a) The effect of increasing rates of phosphorylation by increasing [ATP]/[ADP] = E, on the initial rates of total net influx of external label, $A_1 = 25$ mM into the intracellular free sugar pool: initial $A_2 = 0$ and hexose phosphate pool, initial $B_2 = 0$ and net exit from preloaded cells with isotopic label, $C_2 = 25$ mM cells. Net flux = (influx − efflux) is also shown. The initial intracellular [hexose phosphate] of isotope $B_2 = 0$ and $D_2 = 1$ mM. The exchange rate constant, e, is 5000 s^{-1}, and intersite mobility constant, k, is 500 s^{-1}.

(b) The conditions shown in this figure are the same as in Fig. 7a, except that the exchange rate, e, is zero.

phate, D_2, and only one form is present in the external solution, free sugar, A_1.

The line labelled 'influx' is a plot of total sugar inflow of A_1 into the cytosolic pools of free sugar, A_2, and hexose phosphate, B_2. The line labelled 'efflux' is the exit of free sugar, C_2, from the internal pool into the external solution, C_1. This is equivalent to unidirectional exit. The line labelled 'net uptake', is the difference between the influx and efflux.

When the phosphorylation rate is slow, and the transporter is capable of rapid exchange (Fig. 7a), net flux is minimal and both unidirectional influx and efflux are observed to be approximately equal. Increasing the phosphorylation rate, by raising $E = [ATP]/[ADP]$, increases unidirectional sugar influx to a maximum and also reduces unidirectional efflux. Both these effects result from depletion of sugar ligands, A_2 and C_2, bound to the inner sites. With high rates of phosphorylation, exchange influx and efflux decrease as the proportion of inner sites binding sugar is diminished. In contrast to unidirectional influx, net flux increases continuously to a maximum. Unidirectional influx and net influx reach equality at very high rates of phosphorylation, when both the exchange flux and efflux components are negligible.

The only difference between Figs. 7a and 7b is the absence of a rapid exchange in Fig. 7b. In Fig. 7b, unidirectional influx only exceeds net influx when phosphorylation rates are negligible.

High rates of exchange are only observed when the free sugar concentration inside the cell is sufficiently high and when the membrane-bound kinase activity is sufficiently low to permit a high proportion of the sites on both surfaces to be occupied by sugar. These graphs provide an explanation for the finding that in yeasts, exchange flux is observed mainly at low temperatures [13,14], when the metabolic rate is low and also explains why metabolic inhibition accelerates unidirectional exit of intracellular free sugar via the transport system [10].

Influence of the distribution of the kinase reaction between membrane and cytosol on transport

The main theme of this paper has been the use of a transport system loosely coupled to metabolism to explain stationary state accumulation of an incompletely metabolized sugar.

Although this phenomenon has didactic importance, it has little physiological significance.

However, transference of hexokinase activity

from the cytosol to the membrane, or increased accessibility of the sugar bound at the inner membrane surface to cytosolic hexokinase, would accelerate uptake of a transported and metabolized ligand and retard free sugar exit from the cytosolic pool. This effect could have two advantages over the tandem transport process [5,6]:

(1) The maximal velocity of net sugar uptake would be increased, even when the cytosolic concentration of transported ligand is close to, or above that in the external solution. This would buffer the cytosolic substrate pool against the effects of transient decreases in the external substrate concentrations.

(2) High rates of inflow are possible, even when the transport system has a high affinity for the substrate and there is sufficient free substrate present within the cytosol to inhibit passive net transport completely. When phosphorylation of the transported ligand occurs on the inner surface, it is advantageous to have substrates with high affinity for the transport system, as slippage is reduced and hence the efficiency of coupling increased.

Appendix

Matrix solutions for steady-state flows through networks

The six possible states of the two site pore, shown in Figs. 2e and 2g; the possible transformations between states and rates of these transformations can be represented in matrix form. The fractional occurrence of any of the six states, N_i, may be expressed as a probability, N_i. The sum of the probabilities of all six states

$$\sum_i N_i = 1$$

At steady state, the inflows and outflows to and from any state, N_i are equal.

Hence, for the empty state, N_0

$$dN_0/dt = N_1 \cdot w + N_2 \cdot z + N_3 \cdot w - N_0 \cdot (A_1 \cdot x + B_2 \cdot y + A_2 \cdot x) = 0 \qquad \text{(A1)}$$

where w and z are the first-order dissociation constants of ligands A and B, and $A_1 \cdot x$; $A_2 \cdot x$ and $B_2 \cdot y$ are the pseudo-first-order association constants of ligand binding to vacant sites.

The six equations for each membrane state may be solved simultaneously for the steady-state condition [43].

As the total number of sites is invariant, only five of the six equations are independent. If a unity vector is substituted in any row, the solution of the set of equations represents the fractional proportion of each state.

In the matrix representation of the six state network in Table Ia, each column contains the first-order, or pseudo-first-order rate constants for outflow from the membrane state, given by the column number, to each state, given by the row number. Thus at the matrix position; column 0, row 1, there is the pseudo-first-order association constant, $A_2 \cdot x$, which determines the rate of transformation from state $N_0 \rightarrow N_1$ by uptake of sugar, A_2, onto vacant sites at the inner surface. Similarly, at matrix position; column 1, row 0, there is the first-order constant determining the rate of dissociation of sugar from the inner sites, which gives the rate of transformation of state $N_1 \rightarrow N_0$. Empty spaces (·) indicate that no transformation can be made between the states in a single step. On each of the main diagonal positions of the matrix (marked by stars) is the negative sum of all the outflows from the state denoted by the row number, into all the other possible states. These constants are shown in the table at the side of each row. Hence the rate of outflow of

TABLE Ia

THE SIX-STATE NETWORK (Figs. 2e AND 2g) IN SHORTHAND MATRIX NOTATION

Each row contains the first-order or pseudo-first-order rate constants which transform the state given by row number into the membrane state given by the column number. The main diagonal position of the matrix (marked by stars) is the negative sum of all the possible outflows from the state denoted by the row number.

	0	1	2	3	4	5	
0	★	w	z	w	.	.	$0,0 = -(A_2x + B_2y + A_1x)$
1	A_2x	★	p	k	w	.	$1,1 = -(w + Es + k + A_1x)$
2	B_2y	Es	★	.	.	w	$2,2 = -(z + p + A_1x)$
3	A_1x	k	.	★	w	z	$3,3 = -(w + k + A_2x + B_2y)$
4	.	A_1x	.	A_2x	★	p	$4,4 = -(w + w + Es)$
5	.	.	A_1x	B_2y	Es	★	$5,5 = -(w + z + p)$

TABLE Ib

THE MATRIX REPRESENTATION OF THE FIFTEEN-STATE NETWORK SHOWN IN Fig. 3.

C is an isotopic form of free sugar, A, and D is the isotopic form of hexose phosphate, B. Free sugar A transforms to B, and free sugar C transforms to hexose phosphate D. The isotopes have identical association and dissociation constants and they are treated in an identical way by hexokinase. The only additional rate constant required is the exchange constant 'e' which is the rate of exchange between forms N_7 and N_5.

	0	1	2	3	4	5	6	7	8	9	10	11	12	13	14	
0	★	w	w	w	.	.	w	.	.	z	.	.	z	.	.	$0,0 = -(A_1x + C_1x + A_2x + C_2x + B_2y + D_2y)$
1	A_1x	★	.	k	w	.	.	w	.	.	z	.	.	z	.	$1,2 = -(w + k + A_2x + k + C_2x + B_2y + D_2y)$
2	C_1x	.	★	.	.	w	k	.	w	.	.	z	.	.	z	$2,2 = -(w + A_2x + k + C_2x + B_2y + D_2y)$
3	A_2x	k	.	★	w	w	.	.	.	p	.	.	.	.	.	$3,3 = -(w + k + A_1x + C_1x + Es)$
4	.	A_2x	.	A_1x	★	.	.	.	.	.	p	.	.	.	.	$4,4 = -(w + w + Es)$
5	.	.	A_2x	C_1x	.	★	.	e	.	.	.	p	.	.	.	$5,5 = -(w + w + e + Es)$
6	C_2x	.	k	.	.	.	★	w	w	.	.	.	p	.	.	$6,6 = -(w + k + A_1x + C_1x + Es)$
7	.	C_2x	.	.	.	e	A_1x	★	.	.	.	.	.	p	.	$7,7 = -(w + e + w + Es)$
8	.	.	C_2x	.	.	.	C_1x	.	★	.	.	.	.	.	p	$8,8 = -(w + w + Es)$
9	B_2y	.	.	Es	.	.	.	.	.	★	w	w	.	.	.	$9,9 = -(z + p + A_1x + C_1x)$
10	.	B_2y	.	.	Es	.	.	.	.	A_1x★		.	.	.	.	$10,10 = -(z + p + w)$
11	.	.	B_2y	.	.	Es	.	.	.	C_1x.		★	.	.	.	$11,11 = -(z + p + w)$
12	D_2y	.	.	.	.	.	Es	.	.	.	.	.	★	w	w	$12,12 = -(z + p + A_1x + C_1x)$
13	.	D_2y	.	.	.	.	.	Es	.	.	.	.	A_1x	★	.	$13,13 = -(z + p + w)$
14	.	.	D_2y	.	.	.	.	.	Es	.	.	.	C_1x	.	★	$14,14 = -(z + p + w)$

N_0 to all other states it determined by: $-N_0 \cdot (A_1x + B_2y + A_2x)$, cf. Eqn. A1. Substitution of the equivalent numerical values for the rate constants shown in the matrix, permits numerical solutions for the fractional probabilities of each state to be obtained in the stationary state condition.

Solutions to these equations were obtained using the Gauss-Seidel iterative method with custom written software.

Once the fractional probabilities of each state

TABLE II

COMPUTER GENERATED TABLES SHOWING THE SOLUTIONS IN TERMS OF FRACTIONAL PROBABILITIES OF OCCURRENCE OF EACH STATE N_0–N_5 (SIX-STATE MODEL), AND N_0–N_{14} (FIFTEEN-STATE MODEL)

TABLE IIa

FRACTIONAL PROBABILITY OF OCCURRENCE OF STATES N_0–N_5 OF THE SIX-STATE MODEL WHEN E = [ATP]/[ADP] IS VARIED. ALSO SHOWN ARE THE RATE OF TOTAL NET SUGAR UPTAKE AND THE RATE OF CONVERSION OF SUGAR INTO HEXOSE PHOSPHATE

The external [sugar], A_1, is 1 mM. The intracellular concentrations of: free sugar, A_2, 14 mM; hexose phosphate, B_2, 1 mM. The association rates of: free sugar, x, and hexose phosphate, y, for vacant sites both are 100 $mM^{-1} \cdot s^{-1}$. The dissociation rate of sugar from sites, w, is 25 s^{-1} and that of hexose phosphate, z, is 100 s^{-1}, hence the K_d of sugar is 0.25 mM and that of hexose phosphate is 1 mM. The rate of intersite mobility, k, is 100 s^{-1}. When there are equimolar concentrations of sugar, hexose phosphate, ATP and ADP, the forward rate of phosphorylation, $s = 130$ and the reverse rate, $p = 0.05$, hence the ratio $s/p = 2600$.

E	Probability						$\mu mol \cdot (ml\ cells)^{-1} \cdot s^{-1}$	
	N_0	N_1	N_2	N_3	N_4	N_5	total net uptake	conversion rate
0.25	$4.77E-3$	$9.62E-2$	$4.52E-2$	$2.89E-2$	$6.08E-1$	$2.17E-1$	−6.73	22.86
2.5	$1.05E-2$	$4.21E-2$	$1.47E-1$	$4.21E-2$	$1.68E-1$	$5.89E-1$	0.00	68.41
25	$1.39E-2$	$7.04E-2$	$2.09E-1$	$4.50E-2$	$1.93E-2$	$7.05E-1$	3.79	85.59
250	$1.49E-2$	$7.59E-4$	$2.20E-1$	$4.51E-2$	$1.94E-3$	$7.17E-1$	4.44	87.81

TABLE IIb

THE FRACTIONAL PROBABILITY OF OCCURRENCE OF EACH OF THE FIFTEEN STATES IN THE FIFTEEN-STATE NETWORK FOR EXCHANGE SHOWN IN Fig. 3, FOR DIFFERENT VALUES OF E = [ATP]/[ADP]

In addition, the net flux and unidirectional fluxes of isotopes, A and C and the rates of phosphorylation of A and C to B and D, respectively. The rate constants are all the same as those shown in Table IIa for the six-state network except that e the rate of exchange between states N_5 and N_7 is 5000 s^{-1}.

E	Probability									
	N_0	N_1	N_2	N_3	N_4	N_5	N_6	N_7	N_8	N_9
0.25	$4.78E-1$	$8.36E-3$	$2.06E-2$	$1.67E-2$	$2.02E-3$	$1.18E-1$	$7.95E-2$	$1.20E-1$	$3.49E-1$	$8.01E-3$
2.5	$1.05E-2$	$1.51E-2$	$2.69E-2$	$4.27E-3$	$1.14E-3$	$3.21E-2$	$3.78E-2$	$3.46E-2$	$1.01E-1$	$1.97E-2$
25	$1.39E-2$	$2.18E-2$	$2.31E-2.$	$6.44E-4$	$2.05E-5$	$2.56E-3$	$6.38E-3$	$6.91E-3$	$9.82E-3$	$2.47E-2$
250	$1.44E-2$	$3.43E-2$	$1.08E-2$	$1.05E-4$	0.00	$1.79E-4$	$6.54E-4$	$1.31E-3$	$4.64E-4$	$2.53E-2$

at steady state obtained, the stationary state flows of ligands across the network via the transport and phosphorylation cycles can be obtained as follows

$$\text{sugar flux} = k \cdot (N_3 - N_1)$$

$$\text{rate of net phosphorylation} = (N_1 + N_4) \cdot E \cdot s - (N_2 + N_5) \cdot p$$

Fifteen-state network for exchange

The solutions for the fifteen-state network are obtained in the same way as for the six-state network. There are fourteen independent equations, the only additional constant required is e, which determines the rate of exchange between states N_5 and N_7 (Table Ib).

Numerical solutions

The numerical data shown in Table IIa are the fractional probabilities of each of the six possible states, when the ratio [ATP]/[ADP] = E is altered. The intracellular concentration of free sugar, A_2 is set at 14 mM to give zero-flow when $E = 2.5$ and the extracellular concentration, $A_1 = 1$ mM. As E increases, the probability of occurrence of states N_1 and N_4 decreases, whilst that of N_2 and N_5 increases. The probability of N_3 remains nearly constant, hence the rate of sugar movement from outside to inside is increased.

The data shown in Table IIb are the fractional probabilities of all of the 15 possible states of the exchange transport network as the ratio [ATP]/[ADP] is increased. In addition, the net and unidirectional rates of sugar uptake and loss and the rates of phosphorylation of the two isotopes are shown.

The relationship between net flux and E is the same for both net and exchange flux solutions.

Acknowledgements

We thank Professor A. Kleinzeller, for useful discussions; N.A.T.O. for a travel grant, which made these discussions possible and Mr. A. Wells and Dr. J. Martin for guidance on efficient solution and use of the matrix equations.

References

1 Kleinzeller, A., Kolinska, J. and Benes, I. (1967) Biochem. J. 104, 843–851
2 Kleinzeller, A., Kolinska, J. and Benes, I. (1967) Biochem. J. 104, 852–860
3 Kleinzeller, A. and McAvoy, E.M. (1976) Biochim. Biophys. Acta 455, 126–143
4 Elsas, L.J. and Macdonell, R.C. (1972) Biochim. Biophys. Acta 255, 948–959
5 Wohlhueter, R.M. and Plagemann, P.G.W. (1980) Int. Rev. Cytol. 64, 171–240
6 Koren, R., Shohami, E. and Yeroushalmi, S. (1979) Eur. J. Biochem. 95, 333–339
7 Foley, J.E. and Gliemann, J. (1981) Biochim. Biophys. Acta 648, 100–106
8 Van Steveninck, J. (1968) Biochim. Biophys. Acta 163, 386–394
9 Van Steveninck, J. (1972) Biochim. Biophys. Acta 274, 575–585
10 Kotyk, A. and Michaljanicova, D. (1974) Biochim. Biophys. Acta 332, 104–113

The initial concentrations:
sugar isotope, A_1 in the external solution, 1 mM
sugar isotope, C_1 in the external solution 0
sugar isotope, A_2 in cytosol, 0
sugar isotope, C_2 in cytosol, 14 mM
hexose phosphate, B_2, 0 and hexose phosphate, D_2, 1 mM

Probability					μmol·(ml cells)$^{-1}$·s^{-1}				
N_{10}	N_{11}	N_{12}	N_{13}	N_{14}	total net flux	total influx of A	Exit of C	Conversion rate	
								A → B	C → D
1.17E−2	3.07E−2	3.72E−2	6.76E−2	1.07E−1	−6.73	8.92	−15.65	5.00	17.66
1.88E−2	8.37E−2	1.28E−1	2.04E−1	2.83E−1	0.0	13.15	−13.16	12.12	55.74
2.03E−2	9.25E−2	1.85E−1	3.19E−1	2.74E−1	3.79	13.87	−10.07	13.65	71.26
2.03E−2	4.52E−2	1.95E−1	5.22E−1	1.29E−1	4.44	9.08	−4.65	9.00	78.12

11 Meredith, S.A. and Romano, A.H. (1977) Biochim. Biophys. Acta 497, 745–759
12 Jaspers, H.T.A. and Van Steveninck, J. (1975) Biochim. Biophys. Acta 406, 370–385
13 Cirillo, V.P. (1968) J. Bacteriol. 95, 1727–1731
14 Kuo, S.C., Christensen, M.S. and Cirillo, V.P. (1970) J. Bacteriol. 103, 671–678
15 Kuo, S.C. and Cirillo, V.P. (1970) J. Bacteriol. 103, 679–685
16 Van Steveninck, J. and Dawson, E.C. (1968) Biochim. Biophys. Acta 150, 47–55
17 Van Steveninck, J. and Rothstein, A. (1965) J. Gen. Physiol. 49, 235–246
18 Franzusoff, A. and Cirillo, V.P. (1982) Biochim. Biophys. Acta 688, 295–304
19 Bisson, L.F. and Fraenkel, D.G. (1983) Proc. Natl. Acad. Sci. USA 80, 1730–1734
20 Spoerl, E. (1969) J. Membrane Biol. 1, 468–478
21 Postma, P.W. and Roseman, S. (1976) Biochim. Biophys. Acta 457, 213–257
22 Schachter, H. (1973) J. Biol. Chem. 248 ,974–976
23 Thompson, J. and Chassy, B.M. (1985) J. Bacteriol. 162, 224–234
24 Kundig, W. and Roseman, S. (1971) J. Biol. Chem. 246, 1407–1418
25 Stock, J.B., Weygood, E.B., Meadow, N.B., Postma, P.W. and Roseman, S. (1982) J. Biol. Chem. 257, 14543–14552
26 Pritchard, J.B., Booz, G. and Kleinzeller, A. (1978) Am. J. Physiol. 234, F424–F431
27 Naftalin, R.J. and Kleinzeller, A. (1981) Am. J. Physiol. 240, G392–G400
28 Broun, G., Thomas, D. and Selegny, E. (1972) J. Membrane Biol. 8, 313–332
29 DeSimone, J.A. and Caplan, S.R. (1973) Biochemistry 12, 3032–3044
30 Bunow, B. (1978) J. Theoret. Biol. 75, 51–78
31 Hill, T.L. and Kedem, O. (1966) J. Theoret. Biol. 10, 399–441
32 Pietrobon, D. and Caplan, S.R. (1985) Biochemistry 24, 5864–5776
33 Lieb, W.R. and Stein, W.D. (1974) Biochim. Biophys. Acta 373, 178–196
34 Naftalin, R.J. and Holman, G.D. (1977) in Membrane Transport in Red Cells (Ellory, C. and Lew, V.A., eds.), Academic Press, London
35 Naftalin, R.J., Smith, P.M. and Roselaar, S.E. (1985) Biochim. Biophys. Acta 820, 235–249
36 Veech, R.L. (1979) J. Biol. Chem. 254, 6538–6547
37 Zoratti, M., Pietrobon, D. and Azzone, G.F. (1982) Eur. J. Biochem. 126, 443–451
38 Kedem, O. and Caplan, S.R. (1965) Trans Faraday Soc. 61, 1897–1911
39 Morowitz, H.J. (1966) J. Theoret. Biol. 13, 60–62
40 Klein, M.J. (1955) Phys. Rev. 97, 1446–1448
41 Hill, T.L. (1977) Free energy transduction in Biology: Steady-state Kinetics and Thermodynamic Formalism, Academic Press, New York
42 Hill, T.L. and Eisenberg, E. (1981) Q. Rev. Biophys. 14, 463–511
43 King, E.L. and Altman, C. (1956) J. Phys. Chem. 60, 1375–1378